

Single Liquid Aerosol Microparticle Electrochemistry on a Suspended Ionic Liquid Film

Lynn E. Krushinski, Kathryn J. Vannoy, and Jeffrey E. Dick*

Liquid aerosols are ubiquitous in nature, and several tools exist to quantify their physicochemical properties. As a measurement science technique, electrochemistry has not played a large role in aerosol analysis because electrochemistry in air is rather difficult. Here, a remarkably simple method is demonstrated to capture and electroanalyze single liquid aerosol particles with radii on the order of single micrometers. An electrochemical cell is constructed by a microwire (cylindrical working electrode) traversing a film of ionic liquid (1-butyl-1-methylpyrrolidinium bis(trifluoromethylsulfonyl)imide) that is suspended within a wire loop (reference/counter electrode). An ionic liquid is chosen because the low vapor pressure preserves the film over weeks, vastly improving suspended film electroanalysis. The resultant high surface area allows the suspended ionic liquid cell to act as an aerosol net. Given the hydrophobic nature of the ionic liquid, aqueous aerosol particles do not coalesce into the film. When the liquid aerosols collide with the sufficiently biased microwire (creating a complex boundary: aerosol|wire|ionic liquid air), the electrochemistry within a single liquid aerosol particle can be interrogated in real-time. The ability to achieve liquid aerosol size distributions for aerosols over 1 µm in radius is demonstrated.

1. Introduction

The chemical composition of aerosols is extremely dynamic, contributing to local and global air quality and climate.^[1] The chemistry confined in these liquid aerosols plays a vital role in environmental processes, and their pollution impacts public health.^[2] In laboratory conditions, sprayed microdroplets have been shown to have surprising reactivity,^[3] where unique properties of the

L. E. Krushinski, K. J. Vannoy Department of Chemistry Purdue University West Lafayette, IN 47907, USA I. E. Dick

Elmore Family School of Electrical and Computer Engineering Purdue University

West Lafayette, IN 47907, USA E-mail: jdick@purdue.edu

The ORCID identification number(s) for the author(s) of this article can be found under https://doi.org/10.1002/smll.202308637

© 2024 The Authors. Small published by Wiley-VCH GmbH. This is an open access article under the terms of the Creative Commons Attribution License, which permits use, distribution and reproduction in any medium, provided the original work is properly cited.

DOI: 10.1002/smll.202308637

liquid|air interface are implicated as the driving force for important reactions.[4] In recent years, especially, accelerated/spontaneous redox reactions have been observed[5] in microdroplets, and the electric field at the interface of two dielectrics (air|water) is often suggested to contribute. Verlet's group found that the photooxidation reaction forming the phenolate anion is 2-4 times faster at the boundary compared to bulk.[6] Photochemistry has also been shown to generate hydroxyl radicals, which may drive various oxidation reactions;[7] other groups suggest that the water air interface of microdroplets can produce hydroxyl radicals without the added energy from light or heat.[8]

Electrochemistry is a promising technique for the analysis of single aerosols, as it has been used for the analysis of a wide variety of single entities, [9] including emulsion nanodroplets. [10] In these reports, the microdroplet interface is water|oil, and ions traverse the liquid–liquid boundary to maintain electroneutrality, allowing

electroanalysis of micro- and nanodroplet contents. Accelerated reactivity of aqueous microdroplets suspended in oil was studied previously where droplets collided with a working microelectrode submerged in an emulsified solution. [10e] However, when deployed for the analysis of liquid aerosols, electrochemistry is limited by the necessity for a complete electrochemical circuit, requiring communication between the working and counter/reference electrodes.

We have previously addressed this limitation by using particleinto-liquid sampling techniques, where a collector volume dissolves liquid aerosols and their contents.[11] While this is a promising technique that has demonstrated low limits of detection (≈100 µm for lead),[11a] it still involves dilution of analyte and the inability to access analysis of intact, individual liquid aerosols. While our lab has reported other electrochemical aerosol analysis methods to circumvent particle-into-liquid sampling methods, these techniques require the construction of a dual barrel micro- or nanoelectrode, where a single liquid aerosol must bridge the two electrodes (in current fabrication, electrode distance is >10 µm).[12] These geometric constraints dictate the size of the single aerosols measurable and the timescale for analysis before reactions at one electrode impact the measurement at the other. To increase the aerosol collection efficiency and avoid geometric complications, we www.advancedsciencenews.com

SMQ www.small-journal.com

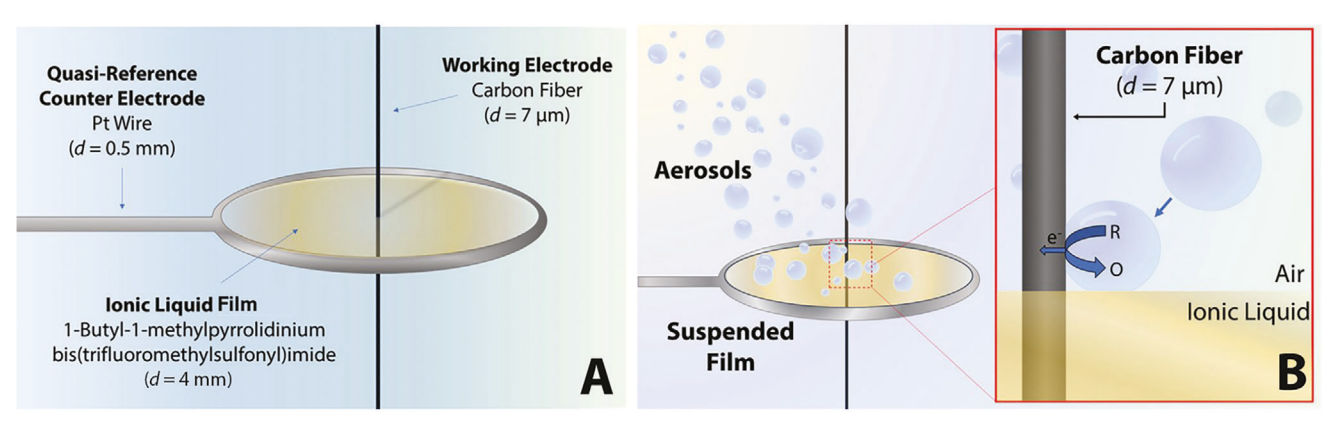


Figure 1. A) Schematic of the electrochemical cell used for aerosol capture and electroanalysis. A malleable platinum wire (d = 0.5 mm) formed a loop ($d \approx 4$ mm) that contained suspended ionic liquid. The platinum wire acted as both a support and quasi-reference electrode. The working electrode is a carbon fiber (d = 7 µm) that traverses the ionic liquid film. B) Schematic of the aerosol experiment with magnified view of the electrochemical reaction occurring within a single liquid aerosol: O is the oxidized species, which donates an electron at the microwire surface to form the reduced species, R.

previously developed a detection scheme where two wires were pushed through a soap bubble wall and used as the working and reference/counter electrodes. The resulting electrochemical cell was used to detect methamphetamine from sprayed aerosols. $^{[13]}$ Though particle-into-liquid sampling likely occurred, the surface area of the 18 μm -thick soap bubble wall maximized collection while minimizing dilution of the analyte. However, these aqueous films evaporated readily, and "popped" on the order of tens of seconds.

Here, we present a simple two electrode cell to measure single micrometer-sized liquid aerosols: a carbon fiber working electrode passes through an ionic liquid film, which is supported by a platinum wire loop that acts as the counter/reference electrode. This novel electrochemical cell allows for the capture and analysis of single liquid aerosols without significant analyte dilution and presents a more readily deployable aerosol analysis system. This construct is the first robust demonstration of liquid aerosol stochastic electrochemistry. We use concepts in stochastic electrochemistry to build an aerosol size distribution, which lies within a distribution of microdroplets measured by light scattering techniques for aerosol particles larger than 1 µm in radius. At present, this is the only electrochemical technique to access chemistry in true microdroplets, where a majority of the microdroplet interface is aquoues|air.

2. Results and Discussion

2.1. Construction of the Electrochemical Cell

As we mentioned before, bubbles are advantageous, but they often pop. An ionic liquid film was used because of the negligible vapor pressure nature of the ionic liquid, preserving a robust film over long periods of time. In our experimental setup, the ionic liquid bubble was observed to survive over at least three weeks. The construction is simple and robust, requiring no specialized instruments to fabricate, and ionic liquid is a non-toxic, environmentally friendly solvent, suggesting this platform could be field-deployable. The use of a hydrophobic ionic liquid (1-butyl-1-methylpyrrolidinium

bis(trifluoromethylsulfonyl)imide) suspended film allows for the capture of aqueous liquid aerosols without dilution of hydrophilic analytes.

To capture and analyze liquid aerosols, an electrochemical cell was constructed, where a carbon fiber working electrode passed through a suspended ionic liquid film supported by a platinum (Pt) wire loop. This loop acted as a quasi-reference and counter electrode. The resulting effective working electrode is a baseless cylinder with a length dictated by the height of the suspended ionic liquid film. A schematic of this electrochemical cell be seen in Figure 1 and images of the actual experimental set-up can be seen in Figures S1 and S2, (Supporting Information). The diameter of the carbon fiber was measured to be 7 µm by scanning electron microscopy (Figure S3, Supporting Information). In this work, the wetting of the carbon fiber was limited by carefully threading the working electrode through a small opening in the platinum wire loop (Figure S1B, Supporting Information) via a micro-positioner. This method was used to minimize unintentional wetting and ionic liquid contamination along the wire. To further characterize the electrochemical cell, ferrocenemethanol, a hydrophobic (relative to hexacyanoferrate(II/III) and hexaamineruthenium(II/III), see below) one-electron mediator was dissolved into the ionic liquid and cyclic voltammetry was performed. The diffusion coefficient of ferrocenemethanol in the ionic liquid was determined by bulk voltammetry (Figure S4, Supporting Information). A finite element simulation was used to model the system. Neglecting wetting along the microwire, the model is designed with a homogenous thickness across the film. From the optical microscopy (Figure S2, Supporting Information), the wetting geometry is insignificant compared to the ionic liquid thickness. This allows only one adjustable parameter: the film thickness/the length of the microwirelionic liquid boundary (Figure S5, Supporting Information), which was fit to experimental data to extract a value of 250 µm. Given the thickness of the ionic liquid film, the total current measured electrochemically is insensitive to the geometry of how the ionic liquid film wets the carbon fiber wire. Figure S6 (Supporting Information) shows that the computation fits the experimental voltammetry well with these assumptions.

nditions) on Wiley Online Library for rules of use; OA articles are governed by the applicable Creative Commons

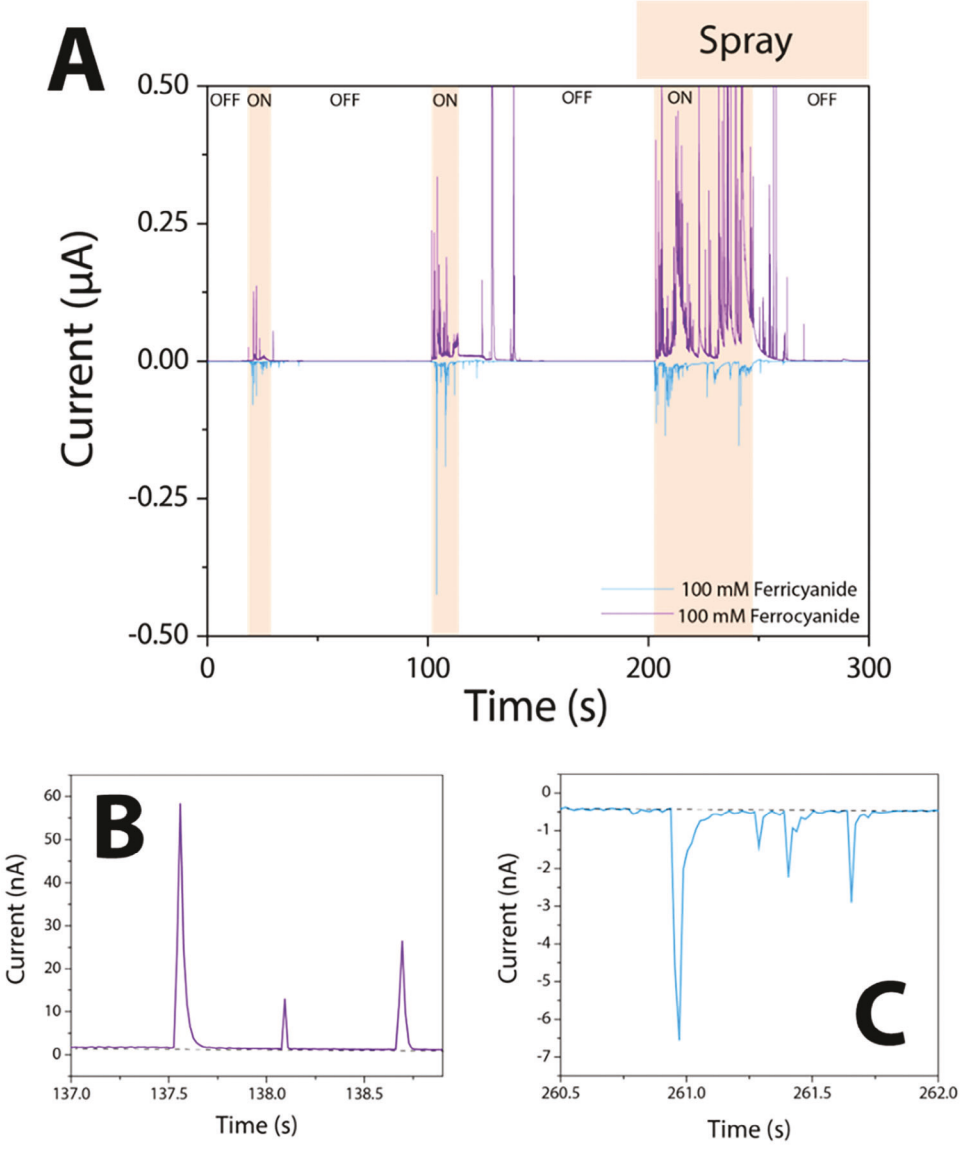


Figure 2. A) Amperograms obtained in an ionic film electrochemical cell while an aqueous solution containing an electroactive mediator was nebulized into a mist. Nebulization occurred only in the highlighted timepoints (20–30 s, 100–110 s, 200–230 s). The blue trace shows an amperogram where 100 mm potassium hexacyanoferrate(III) was nebulized, and the working electrode was biased at -0.5 V versus platinum wire. The purple trace shows an amperogram where 100 mm potassium hexacyanoferrate(II) was nebulized, and the working electrode was biased at +0.5 V versus platinum wire. In both cases, amperometry was performed for 300 s with a sample interval of 0.0167 s. The working electrode was a carbon fiber ($d = 7 \mu m$) and the quasi-reference counter electrode was the platinum wire support. B) Zoom-in on representative transient events during 100 mm potassium hexacyanoferrate(III) amperometry in panel A. C) Zoom-in on representative transient events during 100 mm potassium hexacyanoferrate (III) nebulization experiment panel A. For all panels in this figure, IUPAC convention is used, where anodic current is plotted as positive and cathodic current is represented as negative.

2.2. Electrochemical Collision Experiments with Liquid Aerosols

After set-up of the electrochemical cell, amperometry was performed during nebulization of water containing 100 mm potassium hexacyanoferrate(II) or 100 mm potassium hexacyanoferrate(III). In these experiments, the carbon fiber working electrode is biased such that the electroactive mediator in the aerosol droplet will be oxidized or reduced and give rise to a current response when an aerosol droplet makes contact with both the biased microwire and the film (Figure 1B). Aerosol droplets

contacting only the ionic liquid film will not be detected, though microdroplets contact only the microwire can impart a negligible charge (Figure S7, Supporting Information, discussed further below). The current–time traces are given in Figure 2A–C and show the typical transient responses of single liquid aerosol collision events of hexacyanoferrate(III) and hexacyanoferrate(II) containing aerosols, respectively. Here, we applied a potential sufficient to drive mass-transfer limited (maximum rate) electrolysis within the aerosol as it meets the electrode, but insufficient to drive significant rates of water or ionic liquid oxidation or

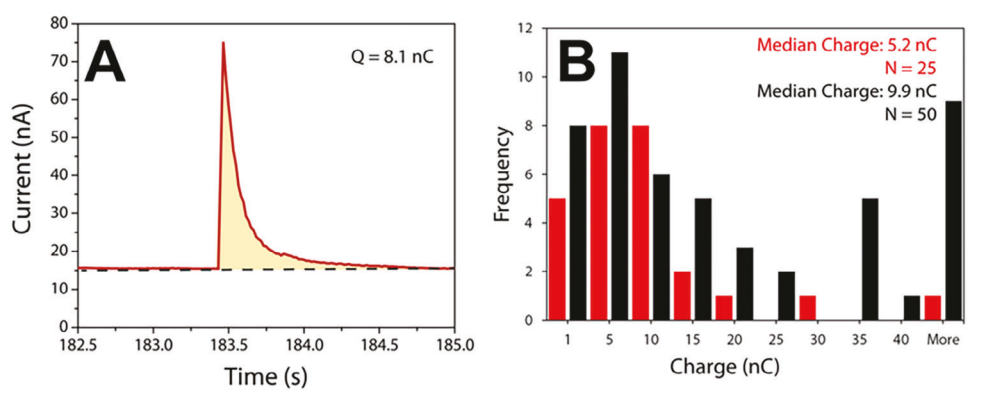


Figure 3. A) Representative collision transient during 100 mm potassium hexacyanoferrate (II) nebulization. The dashed line is the baseline, the integrated peak area is given in yellow, and the measurement of total charge, *Q*, is inset. B) Histograms of the charge passed from single aerosol collision events during (red) and after (black) nebulization of 100 mm potassium hexacyanoferrate (II). For all panels in this figure, IUPAC convention is used, where anodic current is represented as positive.

reduction, such that the measured current reports on the consumption of the analyte within the liquid aerosol droplet.

Collision events can be seen even after the nebulization of the analyte solution has stopped. Replicate amperometry (Figure S8, Supporting Information) during nebulization of 100 mm hexacyanoferrate(II), shows this observation is consistent. We have also observed this with other analyte species (hexaamineruthenium (III)) (Figure S9, Supporting Information). This may be due to aerosols with longer atmospheric lifetimes,[14] but from Video S1 (Supporting Information) the effect may also be due to aerosols that are captured by the ionic liquid film during spray and move toward the working electrode after the nebulization has stopped. At this time, we do not know the details of the adsorbed droplet movement, but we suggest it may be due to evaporative convection and/or a capillary effect. Video \$1 (Supporting Information) shows 100 mm hexacyanoferrate(II) liquid aerosols are observed by optical microscopy and appear to move toward the working electrode when the nebulization stops and the local humidity decreases. The high ionic strength of potassium hexacyanoferrate(II) allows these liquid aerosols to resist evaporation and dissolution into the ionic liquid bubble wall such that they remain intact and loaded with the electroactive species. Video S2 (Supporting Information) shows less obvious accumulation of aerosols along the working electrode after nebulization of 100 mм hexacyanoferrate(III).

We have previously reported the electrochemical response of aerosols when in contact with a wire (a system that closely mimics the carbon fiber herein). When charged liquid aerosols impact the biased electrode, charge transfer occurs because of the differences in electrochemical potential between the two phases. In a control experiment, when we nebulize water droplets (see Figure S6, Supporting Information), transients are still observed in the amperometric *i*–*t* curve. Importantly, these transients are orders of magnitude lower in magnitude than when the liquid aerosol droplet has a redox mediator. These observations indicate that the large responses in the amperometric *i*–t curve are due to faradaic reactions occurring in liquid aerosol droplets. Our further analysis using Faraday's Law also offers supportive evidence of our claim (*vide infra*).

2.3. Electroanalysis of Liquid Aerosol Collisions

Figure 3A shows a typical current transient, which was integrated to give the charge (Q) passed during a discrete collision event. Only transients that were characteristic of an inelastic collision (i.e., a sharp increase in current followed by an exponential decay back to the original baseline) were analyzed. If liquid aerosol particles were disconnecting, an abrupt signal loss would be observed, changing the decay curve. This type of event was rarely seen. Figure 3B shows the distribution of the charge passed for analyzed discrete collision events during (red) and after (black) the nebulization of 100 mm hexacyanoferrate(II). The diameter of the liquid aerosol responsible for each collision event was then calculated from the charge (the integral of the current vs. time response), which is proportional to the total moles of analyte within the aerosol through Faraday's Law. The aerosol diameter ($d_{particle}$) was determined using Equation 1, [10c]

$$d_{particle} = 2 \sqrt[3]{\frac{3Q}{4\pi n F C_{redox}}}$$
 (1)

where Q is the integrated charge (C, coulombs), n is the number of electrons transferred per molecule (1 for hexacyanoferrate(II)), F is Faraday's constant (96 485 C mol⁻¹), and C_{redox} is the concentration of the redox molecule in the microdroplet (100 mm).

The liquid aerosol size distributions during and after spray based on Equation 1 are shown in **Figure 4** (green and blue bars, respectively), where the particle diameter is the calculated diameter of the nebulized liquid aerosols. The electrochemically calculated distribution was compared to the aerosol size data collected with a Grimm 11-D Aerosol Spectrometer (red trace) at selected particle diameters. It can be seen from Figure 4 that the calculated diameters lie within the distribution of larger ($d > 2 \mu m$) measured liquid aerosols, indicating that the electrochemical response may be reporting on single aerosols. It is important to point out that a drawback of the technique is that it does not account for liquid aerosols that previously coalesced (either in air or, more likely, on the ionic liquid film before reaching the electrode). There is a time and humidity component, as longer times

www.advancedsciencenews.com

NANO · MICRO SMOIL www.small-journal.com

decreases our ability to see discrete liquid aerosol droplet electrochemistry as the pool gets larger. The accuracy of droplet sizes decreases for smaller droplets as the pre-adsorbed aqueous pool increases in size. This is a simple dilution problem: the number of moles entering the aqueous pool from the coalescing liquid aerosol must be large enough to give a high enough concentration to be electrochemically detectable in the pool.

The system as presented is specific for redox capable species. However, manipulations of the system could potentially lead to measurements of non-electrochemically active species (such as electrode functionalization with aptamers^[15] or use of reporter molecules within the ionic liquid film [EC' reactions][16]). If the aerosol contained two electrochemically active species which are oxidized/reduced at similar potentials in water, it would be difficult to deconvolute the measured current transients. However, in the cases of species that are oxidized/reduced at potentials significantly different from one another (10 s-100 s of mV separation), it could be possible to select a specific signal based on the applied potential. Other manipulations could be done to select specific electrochemically active species if necessary (i.e., selecting an ionic liquid with an affinity for the desired molecule, functionalizing the working electrode, or using voltammetry). To demonstrate the generalizability of the method with regard to redox mediators, experiments with hexaammineruthenium(III) chloride were performed, and the results were comparable to those of potassium hexacyanoferrate(III) (see Figure \$9, Supporting Information). In addition, measurements were repeated at a much lower concentration (10 mm hexacyanoferrate(II/III), Figure S11A, Supporting Information), where the current responses retained the same shape, but were lower in magnitude. These measurements were also repeated in a different ionic liquid (1-butyl-3-methylimidazolium hexafluorophosphate), as shown in Figure S11B (Supporting Information).

Particle Sizer 75000 During Spray After Spray After Spray 25000 Particle Diameter (µm)

Figure 4. Histogram of the aerosol diameter calculated from the charge (plotted in Figure 3B) from discrete collisions of aerosols containing 100 mm potassium hexacyanoferrate(II) during (green bars) and after (blue bars) nebulization. The overlaid red trace is the particle size data obtained from a Grimm 11-D aerosol spectrometer.

and higher humidity increase the probability of droplet coalescence along the film, as shown in the electrochemical results in Figures 3B and 4 where liquid aerosols electrolyzed during the nebulization were smaller on average. Additionally, longer times result in more evaporation, though we expect that the electrochemical system will report on the original size (before significant evaporation), as the amount of moles does not change (see Equation 1).

The full particle size distribution of the nebulized liquid aerosols measured by scattering in air is shown in Figure S10 (Supporting Information). From this figure, it is apparent that there are high counts of small liquid aerosols ($d < 2 \mu m$) that are less frequently observed in the electrochemical collision events. This is likely due to coalescence, as mentioned above, and current measurement limitations. In this study, we have \approx 40 pA of background noise, setting the size of the smallest liquid aerosol detectable at \approx 500 nm in radius (as calculated by Equation 1). We can optimize the noise by introducing a well-grounded Faraday cage. Introducing an aperture between the nebulizer and electrochemical cell may also be used to decrease noise and humidity (decreasing coalescence), which could give access to smaller droplets. We would expect solids, such as dust or pollen, to increase the noise level (if their impact on the wire changes the ionic liquid film wire interface, capacitance fluctuations could occur). The introduction of these solids to the system may perturb the ionic liquid film, but we do not expect these events to generate faradaic current, especially at a scale (10 s of nA) that is significant to the measurement. In high humidity/high collision frequency experiments, the electrode becomes covered with pre-adsorbed liquid aerosols and an aqueous pool can form (as evidenced Videos S1 and S2, Supporting Information). If a preadsorbed aqueous pool gets larger, the probability of a liquid aerosol merging with the pool gets higher (assuming a constant flux of liquid aerosols). While the moles electrolyzed will still indicate the original size of the colliding microdroplet, one must measure quickly enough to temporally resolve the merging of single liquid aerosols with the pre-adsorbed aqueous pool. This

3. Conclusion

We developed a simple and robust two-electrode electrochemical method to analyze individual liquid aerosols. A novel electrochemical cell was constructed by an ionic liquid film suspended in a platinum wire support (quasi-reference/counter electrode) with a carbon fiber microwire working electrode traversing the film. Aqueous aerosols were captured and electrolyzed without significant analyte dilution using a hydrophobic ionic liquid suspended film. In this report, single mediator-containing aerosols were sized via integration of the current-time transient resulting from their interaction with the carbon fiber working electrode at the complex phase boundary (fiberlionic liquid|water|air). We show that while the size distributions of aerosols during and after spray both lie within the size distribution measured by a spectrometer, aerosols that collided during active spray were more reliably sized as opposed to those that were analyzed after the spray was halted. Aerosols that are captured on the ionic liquid film may still be measured when they move to the carbon fiber working electrode but are generally larger when electrochemically sized. This is likely due to the coalescence of droplets on the ionic liquid film which cannot be discounted in the reported experimental conditions. Regardless, we have demonstrated the ability of the presented electrochemical method to analyze discrete liquid aerosols maintaining their water air interface with



www.advancedsciencenews.com

NANO · MICRO SMOIL

www.small-journal.com

unprecedented simplicity, extending the reach of stochastic electrochemistry of microdroplets to liquid aerosols of micrometer dimensions. These measurements present a significant advancement not only toward the deployable sensing of single liquid aerosols but also toward more robust understanding of curious chemistry at the air water interface.

4. Experimental Section

Chemicals and Materials: Potassium hexacyanoferrate(II) trihydrate (potassium ferrocyanide, 99+%, for analysis) and potassium hexacyanoferrate(III) (potassium ferricyanide, 99+%, ACS reagent) were purchased from Thermo Scientific. 1-Butyl-3-methylimidazolium hexafluorophosphate (BMIM-PF₆, for catalysis, \geq 98.5%), 1-butyl-1-methylpyrrolidinium bis(trifluoromethylsulfonyl)imide (BMP-BTI, >99%, <500 ppm H₂O), Hexaammineruthenium(III) chloride (98%) were purchased from Sigma–Aldrich. Millipore water (Millipore Milli-Q, 18.20 M Ω cm $^{-1}$) was used to prepare aqueous solutions.

Electrochemical Cell Set-Up and Ionic Liquid Film Preparation: To create the carbon fiber "floss-picks," electrical wire was stripped, cut, and assembled into a floss-pick like conformation by wrapping two wires around one another and leaving ≈1 cm of each wire free. The wires were secured in place with hot glue. The free ends of the wires were then dipped in gallium (stored at 55 °C to maintain a liquid state) and a carbon fiber (d =7 μm P-55 pitch based fibers, Thornell) was placed between the two wires secured ensuring contact with the gallium. The fibers were then secured in place with a drop of hot glue. An image of the fabricated carbon fiber floss-picks can be seen in Figure S1A (Supporting Information). The flosspick was then held by a clamp and connected to the working electrode lead of a CHI 601E potentiostat. The platinum wire support was fabricated by wrapping ≈6 cm of Pt wire (0.5 mm diameter, 99.9% metals basis, Sigma-Aldrich) around a 0.5 cm circular support to create a bubble wand shape. The copper tape was wrapped around the handle portion of the Pt wire support to create a more stable connection to the leads of the potentiostat. The circular portion of the Pt wire support was then cut with wire cutters directly across from the handle. An image of the fabricated Pt wire support can be seen in Figure S1B (Supporting Information). The ionic liquid suspended film was formed by submerging the Pt wire support into a well on a ceramic well-plate containing the ionic liquid (BMP-BTI). The Pt wire support containing ionic liquid was attached to a Sutter MPC-200 micro-positioner and connected to the reference and counter electrode leads of the potentiostat. The Pt wire support containing ionic liquid was then moved to the carbon fiber floss-pick with the micro-positioner such that the carbon fiber was threaded through the slit on the Pt wire support and traversed the ionic liquid suspended film. Images of the experimental set-up can be seen in Figure S2 (Supporting Information). All voltammetry was performed within a well-grounded Faraday cage within a fume

Aerosol Electroanalysis: Solutions of 100 mm potassium hexacyanoferrate(II) and potassium hexacyanoferrate(III) were prepared in Millipore water. All solutions were nebulized with a Aeroneb Solo Nebulizer connected to a Aeroneb Pro-X controller purchased from Aerogen. A new mesh nebulizer was used for each solution. The Pt wire support was cleaned with acetone and Millipore water between experiments. A new carbon fiber "floss-pick" and fresh ionic liquid film were used for each experiment. For each amperometric i-t experiment, amperometry was run for 300 total seconds, where background amperometry in the ionic liquid film was taken for $\approx\!20$ s before solution nebulization. The solution was then nebulized for $\approx\!10$ s, with the nebulizer held $\approx\!2$ in. from the electrochemical cell. At 100 s, nebulization was repeated for an additional ($\approx\!$) 10 s. At 200 s, nebulization was repeated for $\approx\!30$ s. Sizing of the liquid aerosols was performed with a Grimm 11-D Aerosol Spectrometer and electroanalytical techniques.

Statistical Analysis: All amperograms collected were analyzed as-is (no normalization or transformation was performed). Each amperogram was

screened for current transients which were representative of a temporally resolved event. Examples of transients that demonstrate this ideal behavior as well as examples of those not used for analysis as they deviated from this behavior are seen in Figure S12 (Supporting Information). Transients were integrated using the same CHI Electrochemical Software used for data acquisition and values were recorded in Excel, where histograms of the integrated current (and resultant calculated diameter) were created. For each histogram, a sample size of at least 25 was used. No further statistical analysis was performed.

Supporting Information

Supporting Information is available from the Wiley Online Library or from the author.

Acknowledgements

L.K. and K.J.V. contributed equally to this work. Research reported in this publication was supported by the Chemical Measurement and Imaging Program in the National Science Foundation Division of Chemistry under Grant CHE-2003587/2319925. K.J.V. acknowledges the National Institute of Justice for fellowship support under Grant 2020-R2-CX-0036.

Conflict of Interest

The authors declare no conflict of interest.

Data Availability Statement

The data that support the findings of this study are available from the corresponding author upon reasonable request.

Keywords

aerosols, air, collision electrochemistry, ionic liquid, microdroplets, nanoimpact, suspended film, water interface

Received: September 27, 2023 Revised: December 28, 2023 Published online:

- J. H. Seinfeld, C. Bretherton, K. S. Carslaw, H. Coe, P. J. DeMott, E. J. Dunlea, G. Feingold, S. Ghan, A. B. Guenther, R. Kahn, I. Kraucunas, S. M. Kreidenweis, M. J. Molina, A. Nenes, J. E. Penner, K. A. Prather, V. Ramanathan, V. Ramaswamy, P. J. Rasch, A. R. Ravishankara, D. Rosenfeld, G. Stephens, R. Wood, *Proc. Natl. Acad. Sci. U.S.A.* 2016 113 5781
- [2] Y. Cheng, G. Zheng, C. Wei, Q. Mu, B. Zheng, Z. Wang, M. Gao, Q. Zhang, K. He, G. Carmichael, U. Pöschl, H. Su, *Sci. Adv.* 2016,2, e1601530.
- [3] Z. Wei, Y. Li, R. G. Cooks, X. Yan, Annu. Rev. Phys. Chem. 2020,71,
- [4] a) A. M. Deal, R. J. Rapf, V. Vaida, J. Phys. Chem. A 2021, 125, 4929; b)
 C. M. Dobson, G. B. Ellison, A. F. Tuck, V. Vaida, Proc. Natl. Acad. Sci. U.S.A. 2000, 97, 11864.
- [5] S. Jin, H. Chen, X. Yuan, D. Xing, R. Wang, L. Zhao, D. Zhang, C. Gong, C. Zhu, X. Gao, Y. Chen, X. Zhang, JACS Au 2023, 3, 1563.

SMQ

www.advancedsciencenews.com

www.small-journal.com

- [6] C. J. C. Jordan, E. A. Lowe, J. R. R. Verlet, J. Am. Chem. Soc. 2022, 144, 14012.
- [7] J. M. Anglada, M. T. C. Martins-Costa, J. S. Francisco, M. F. Ruiz-López, J. Am. Chem. Soc. 2020,142, 16140.
- [8] a) K. Li, Y. Guo, S. A. Nizkorodov, Y. Rudich, M. Angelaki, X. Wang, T. An, S. Perrier, C. George, *Proc. Natl. Acad. Sci. U.S.A.* 2023, 120, e2220228120; b) J. K. Lee, K. L. Walker, H. S. Han, J. Kang, F. B. Prinz, R. M. Waymouth, H. G. Nam, R. N. Zare, *Proc. Natl. Acad. Sci. U.S.A.* 2019, 116, 19294.
- [9] a) A. J. Bard, H. Zhou, S. J. Kwon, Isr. J. Chem. 2010,50, 267; b) J. E. Dick, A. T. Hilterbrand, A. Boika, J. W. Upton, A. J. Bard, Proc. Natl. Acad. Sci. U.S.A. 2015,112, 5303; c) J. E. Dick, C. Renault, A. J. Bard, J. Am. Chem. Soc. 2015,137, 8376.
- [10] a) H. Deng, J. E. Dick, S. Kummer, U. Kragl, S. H. Strauss, A. J. Bard, Anal. Chem. 2016,88, 7754; b) J. E. Dick, E. Lebègue, L. M. Strawsine, A. J. Bard, Electroanalysis 2016,28, 2320; c) B.-K. Kim, A. Boika, J. Kim,

- J. E. Dick, A. J. Bard, *J. Am. Chem. Soc.* **2014**,136, 4849; d) B.-K. Kim, J. Kim, A. J. Bard, *J. Am. Chem. Soc.* **2015**,137, 2343; e) K. J. Vannoy, I. Lee, K. Sode, J. E. Dick, *Proc. Natl. Acad. Sci. U.S.A.* **2021**,118, e2025726118.
- [11] a) P. J. Kauffmann, N. A. Park, R. B. Clark, G. L. Glish, J. E. Dick, ACS Meas. Sci. Au. 2022, 2, 106; b) N. A. Park, G. L. Glish, J. E. Dick, J. Am. Soc. Mass Spectrom. 2023, 34, 320.
- [12] P. J. Kauffmann, J. E. Dick, Environ. Sci.: Nano 2023, 10, 1744.
- [13] K. J. Vannoy, N. E. Tarolla, P. J. Kauffmann, R. B. Clark, J. E. Dick, Anal. Chem. 2022, 94, 6311.
- [14] S. Ding, Z. W. Teo, M. P. Wan, B. F. Ng, Build. Environ. 2021,205, 108239.
- [15] J. Kirsch, C. Siltanen, Q. Zhou, A. Revzin, A. Simonian, Chem. Soc. Rev. 2013,42, 8733.
- [16] B. Su, I. Hatay, F. Li, R. Partovi-Nia, M. A. Méndez, Z. Samec, M. Ersoz, H. H. Girault, J. Electroanal. Chem. 2010,639, 102.